Water enriched in the rare stable isotopes

Faghihi, Vahideh

Chapter 2

Adaptation of a gas analyzer based on OF-CEAS (Optical Feedback Cavity Enhanced Absorption Spectroscopy) technology to liquid water isotope measurements in biomedical research

In this chapter, we report on the development of an infrared laser spectrometer based on Optical Feedback Cavity Enhanced Absorption Spectrometry (OF-CEAS) using a distributed feedback diode laser near 1.4 µm. The aim of this instrument is to simultaneously measure the isotopic ratios $^{2}H/^{1}H$, $^{18}O/^{16}O$, and $^{17}O/^{16}O$ in enriched waters for biomedical research. We provide a brief introduction to the technique of OF-CEAS and describe the instrument.

2.1 Introduction

We adapted a near infrared laser spectrometer based on Optical Feedback Cavity Enhanced Absorption Spectroscopy (OF-CEAS) to the simultaneous measurement of the isotopic ratios $^{2}H/^{1}H$, $^{17}O/^{16}O$, and $^{18}O/^{16}O$ in liquid water. The OF-CEAS technique is described in section 2.2.

The laser spectrometer has three parts: a gas phase analyzer that measures the isotopic composition of water vapour, a liquid evaporator to convert liquid water into vapour (hereafter referred to as the flash evaporator), and an autosampler that periodically injects liquid water samples into the evaporator. Figure 1 shows an external view of the spectrometer. The gas analyzer is a modified version of an early prototype spectrometer obtained from the French company AP2E [1]. Its core is in many aspects similar to the instrument described by Landsberg [2]. The opto-mechanics and electronics were left essentially untouched. The laser and the high-reflectivity (cavity ring-down) mirrors were replaced in order to access the desired spectral region for water isotope measurements. The instrument was mounted in a thermally insulated case with dimensions of 80 ×60 ×25 cm^3 and a weight of about 25 kg. The inlet of the analyzer is connected to the flash evaporator, the outlet is connected to a supplementary vacuum pump, and a PC controls the instrument and assures the data processing. We describe each of these parts in sections 2.3 to 2.5. Sections 2.6 to 2.7 are devoted to the measurement procedure, data acquisition, and data analysis.

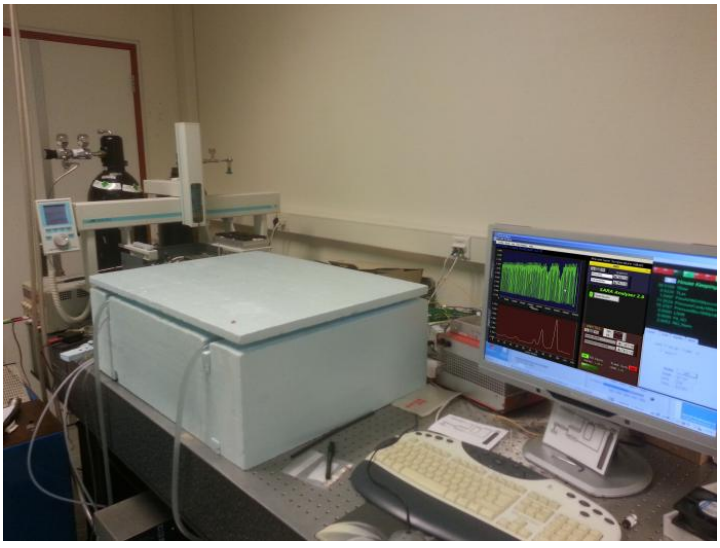

Figure 1. External view of the spectrometer.

2.2 Theory of OF-CEAS operation

We give a brief description of the OF-CEAS technique invented by Morville et al. [3, 4] upon which the commercial prototype instrument described in this chapter is based. We refer to the review by Morvilee and colleagues for more details [5]. In short, OF-CEAS solves the problem of injecting light from a semi-conductor laser into a high-finesse optical cavity by exploiting the sensitivity of most semi-conductor lasers to optical feedback.

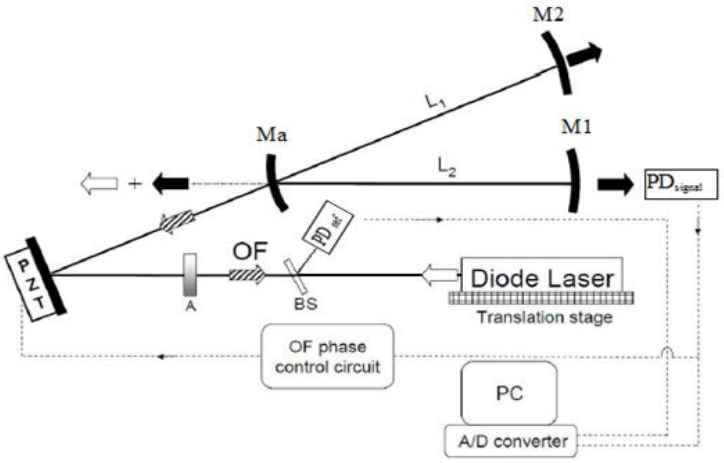

Figure 2. Schematic set-up of OF-CEAS with a V-shaped cavity giving OF when the laser frequency matches the cavity resonance (figure reproduced from [3]). The direct reflection at the input mirror is directed away. M1, M2, and Ma are high-reflectivity mirrors; A is a variable attenuator; BS is a beam splitter; PD_{signal} and, PD_{ref} are the signal and reference photodiode, respectively. The PZT-mounted mirror adjusts the phase of the OF field. See the text for more information.

When the frequency of the laser matches that of a cavity mode, light intensity can build up inside the cavity, some of which is returned toward the laser. If the returned electro-magnetic wave is in phase with the laser output, the field inside the cavity will interfere constructively and intensity will build up. At the same time the laser frequency will self-lock to the transmission frequency of the cavity mode and the laser emission linewidth will narrow to below the width of the cavity mode. Also, when the laser injection current is changed, the laser frequency will initially tune with a tuning rate that is much below that observed for the free-running laser frequency. This reduction of the free-running current tuning rate is controlled by the relative intensity of the optical feedback field: the feedback rate (in our case controlled by rotation of a linear polarizer

between laser and cavity). Morville et al. used a V-shaped cavity consisting of three mirrors. This configuration assures that light returned to the laser (the optical feedback) is necessarily light that has already been spectrally filtered by the optical cavity. Also in this way, direct reflection to the laser from the folding (apex) mirror (Ma in Fig. 2) that could strongly perturb the laser is avoided. The optical feedback phase, the optical feedback rate, and the laser scan rate are crucial parameters, which need to be controlled.

The phase of the optical feedback is controlled in an electronic feedback loop by changing the optical distance between the laser and the cavity with the help of a piezo-actuator-mounted steering mirror between laser and cavity. The error signal for the control loop is derived from a determination of the transmission mode symmetry. Furthermore, the optical distance between laser and cavity is chosen to be (roughly) equal to an integer multiple of the length of the cavity arm that is being directly injected (L1 in Fig. 2). In this way the phase of the optical feedback will not change (noticeably) when the laser frequency is tuned and no intensity modulation (beating) of the cavity transmission maxima is observed.

The feedback rate is another important parameter that needs to be set to an acceptable level. If the feedback rate is too low, sub-optimal filling of the cavity occurs. If, on the other hand, the rate is too high, the range over which the laser frequency remains locked to one cavity transmission mode can become larger than the spacing between successive longitudinal modes (the free spectral range of the cavity), assuming proper spatial mode matching to the TEM_{00} transverse mode of the cavity, causing every other mode to be missing from the cavity transmission spectrum. In the case of poor spatial mode matching of the Gaussian laser beam to the cavity, higher order transverse modes can be inadvertently excited. Finally, we mention that the laser scan rate is another important parameter that is selected such as to allow for sufficient time for the field to build up inside the cavity.

2.3 Gas phase analyzer

The analyzer consists of three main parts: the optical part, the electronic system, and the gas handling part. Figure 3 is a representation of a top view of the gas analyzer of Figure 1.

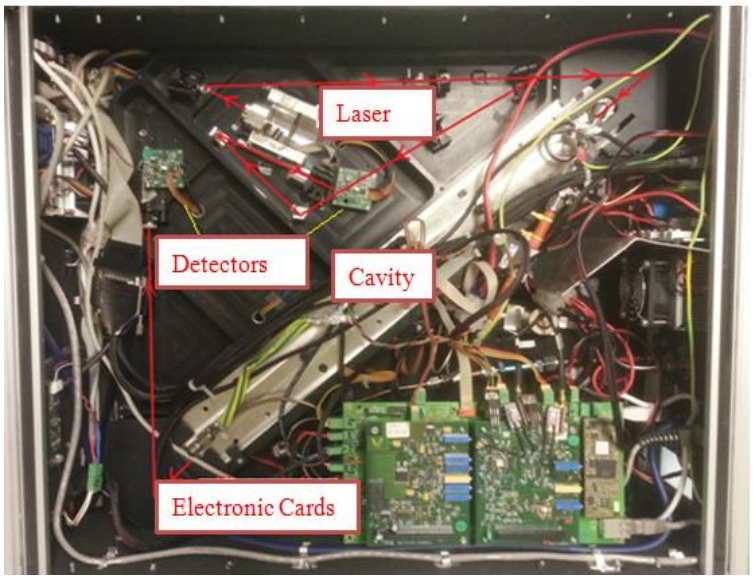

Figure 3. Top view of the gas analyzer casing. Laser beam path indicated in red.

2.3.1 Optical system

The optical part includes the laser, the optical cavity, two detectors, and optical elements (mirrors, lens, beam splitter, polarizer ...), as schematically represented in Figure 2. It is mounted on a triangular base from machined aluminium. This breadboard is mounted on four metallic springs for vibrational isolation. The gas analyzer employs a continuous wave distributed feedback (DFB) diode laser (Laser Components) emitting around 1.4 µm with an output power of 3 mW. The laser is tuned from 7183.5 to 7184.0 cm^{-1}, to probe the absorption lines of the four isotopologues $^{1}H_{2}{}^{18}O$, $^{1}H_{2}{}^{16}O$, $^{1}H_{2}{}^{17}O$ and $^{1}H^{2}H^{16}O$ (Figure 4). The selected region contains a second $^{1}H_{2}{}^{16}O$ line in overlap with two other isotopologues, $^{1}H^{2}H^{16}O$ and $^{1}H_{2}{}^{17}O$, which is included in the spectral fit, but otherwise not used in the analysis. The parameters of the four molecular lines used in the present work are summarized in Table 1. The temperature sensitivity of the isotope ratio (expressed in ‰/K) is to good approximation equal to the difference in temperature coefficients of the rare and abundant isotopologue lines [6] and can to good approximation be calculated using the relationship of Bergamaschi et al.[7]:

$$\frac{\Delta\delta}{\Delta T} \approx \frac{\Delta E}{kT^2} \qquad (1)$$

where ΔE is the difference of ground state energies of the corresponding transitions, k is the Boltzmann constant and T is the absolute temperature.

The selection of the suitable laser wavelength is a key aspect in the instrumental design. Different spectral regions in the infrared range, covered by low-cost and compact DFB lasers, can be selected depending on the measurement requirements [8-12]. It is desirable that the selected absorption lines exhibit similar absorption intensities that are as large as possible (for high sensitivity and accurate measurements), but do not have interference with other species and are well separated from each other to reduce cross-sensitivity, and have similar ground state energy in order to minimize the effects of the temperature dependence of the line intensities. The spectral region near 7184 cm^{-1} (1392 nm) meets these demands, and was for these reasons selected by Kerstel et al. [8]. As can be seen in Figure 4, in the case of an isotopically natural water, the intensity of $^{1}H^{2}H^{16}O$ is significantly lower than that for the other isotopologues. This is actually an advantage in the case of enriched water samples as the ^{2}H enrichment is larger than the ^{18}O and ^{17}O enrichments (enrichment levels are typically up to 16,000 ‰ for ^{2}H and 2,000 ‰ for ^{18}O, and much smaller for ^{17}O; for more details see Chapter 4).

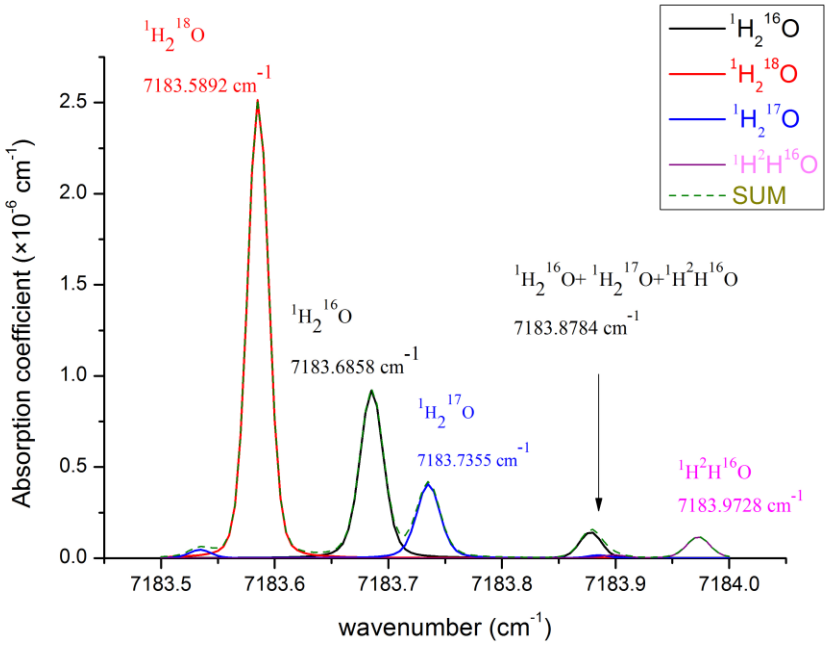

Figure 4. Absorption spectrum around 7184 cm^{-1} simulated for a gas temperature of 296K (i.e., 12 degrees lower than the actual gas cell temperature), a total pressure of 35 mbar, and a volume mixing ratio of water in air of 8500 ppmv using frequencies and Voigt line profile parameters from the HITRAN 2012 database [13].

Table 1. Absorption lines in the selected spectral region. Data from the HITRAN database [13]. The isotope ratio temperature coefficients (TC) were determined using Eq. (1) at the gas cell temperature of 308 K.

Isotopologue	Wavenumber (cm^{-1})	Intensity at 296 K (10^{-23} cm $molecule^{-1}$)	Wavenumber of the lower state of the transition (cm^{-1})	Isotope ratio TC at 308 K (‰ / K)
$H_2{}^{16}O$	7183.6858	0.37	661.5489	ref line
$H_2{}^{17}O$	7183.7355	0.12	94.9705	-8.4
$H_2{}^{18}O$	7183.5859	0.45	733.6829	+1.2
$H^2H^{16}O$	7183.9728	0.034	156.3822	-7.5

The cavity mirrors (from Layertec GmbH) have a radius of 1 m and a wedge angle of 1°. Also, to reduce unwanted reflections, the rear side of the mirrors is anti-reflection coated. These mirrors give an empty-cavity ring down time of τ_0 =20 μs at 1392 nm. This implies a reflectivity of ~ 99.9917 %, a cavity finesse of F~ 19,000, and an effective optical absorption path length of about 6 km, using the formulas for a V-shaped cavity conveniently collected by Landsberg [2]. The V-shaped cavity consists of two arms of about 49.5 cm making an angle of 2 °. The mirrors were glued to metal holders that are fixed to the cavity with an O-ring seal, enabling an easy removal for cleaning without loss of optical alignment. The gas cell with its two internal cavity arms is machined from a single stainless steel block. The instrument has two InGaAs detectors (Hamamatsu) that observe the reference beam and cavity transmission. The distance between laser and cavity is matched to the cavity length, and fine controlled by a piezo-mounted mirror, in order to assure the correct phase of the optical feedback to the laser. The optical path lengths outside the cavity are such that the effect on the recorded spectrum of water absorption occurring outside of the gas cell is minimized.

Three individual electronics cards (AP2E) control the laser current, the laser temperature, and the position of the piezo-mounted mirror, which in turn controls the phase of the optical feedback. The laser temperature was stabilized with a 1-σ accuracy of ~ 3 mK.

2.3.2 The gas handling system

The part of the instrument in contact with the sample gas includes, apart from the optical cavity and gas cell, pressure and flow regulators, pressure and flow sensors and a membrane fixed-speed pump (KNF N813 3ANE). In order to reduce the memory effect due to adsorption of water vapour to the walls of the cavity and inlet tubing, the internal stainless steel surface of the gas cell has been electro-polished and all inlet tubing is fused silica coated ("TrueTube EP", O'Brien). However, PFA tubing (~ 14 cm long) was used between the flash evaporator and the gas analyzer for the purpose of electrical isolation. A Siltek-coated 2-micron filter from Restek has been used before the cavity inlet to prevent contamination from larger particles. The pressure in the cavity is stabilized to 35 mbar in a control loop using a proportional valve (Bronkhorst) (Prop. Valve III in Figure 6) located inside the gas analyzer casing. The flow of water vapour from the flash evaporator to the cavity is regulated with a proportional valve (Bronkhorst) located before the cavity inside the evaporator housing (Prop. Valve II in Figure 6). The flow of ~30 mL/min (STP) is measured with an electronic flow meter (Honeywell AWM3100V) and pressure is measured with an electronic pressure meter (STS ATM 1ST). Both the pressure and flow sensors have been located at the exit of the cavity, which helps to avoid a memory effect due to adsorption of water vapour on the inner walls of the sensors. The cavity temperature is regulated to 35.00± 0.02 °C with a thermo-electric air-to-air heat exchanger (Supercool by Laird Technologies). The laser used in our system emitted the desired wavelength region at temperature of about 7 °C. This prevented us from using the heating bands on the bottom of the optical triangle to set the cavity temperature to a higher value than 35 °C in order to reduce the memory effect, as is done in the other OF-CEAS-based water isotope analyzers [1, 2, 14], as otherwise the thermo-electric cooler of the laser was not able to maintain the laser temperature. Another modification to the standard layout is that we placed an aluminium plate with channels through which water circulates on top of the gas analyzer to lead heat away from the spectrometer housing. Additionally, a fan was used in order to achieve a more uniform air temperature distribution inside the box. In this way, the air temperature inside the entire instrument could be stabilized to 36.01 °C with a 1-σ accuracy of 10 mK. The cavity and air temperature are monitored with calibrated Pt1000 platinum resistors.

2.3.3 Performance of the water isotope analyzer

In order to assess the intrinsic precision of the optical spectrometer, before its shipment from Grenoble to Groningen, a tank was prepared with a mixture of GS-48 water in dry nitrogen to yield a humidity level of 1% (10,000 ppmv). A stable flow of this supply of around 30 sccm through the analyzer's optical cavity was established and data was recorded during about 9 hours. Figure 5 shows the Allan-Werle plot [15] of the 2-sample standard deviation against the averaging time. The minimum standard deviations of 0.26‰ for δ^2H and 0.061‰ for δ^{18}O are obtained after 300 and 500 s, respectively. With an averaging time of 4 minutes, as provided by the liquid water evaporator discussed in section 2.4, the expected level of precision is approximately 0.3‰ and 0.08‰ for δ^2H and δ^{18}O, respectively. The graph lets us also estimate that the attainable precision is degraded by the onset of instrumental drift to reach roughly 0.4‰ and less than 0.08‰ for δ^2H and δ^{18}O, respectively, when the complete measurement including overhead takes 15 min (conform Fig. 7). If this time is extended to 4 hours, such that it encompasses the time required to make 8 repeated injections on both a sample and a reference material, the errors are about 1‰ and 0.2‰ for δ^2H and δ^{18}O, respectively.

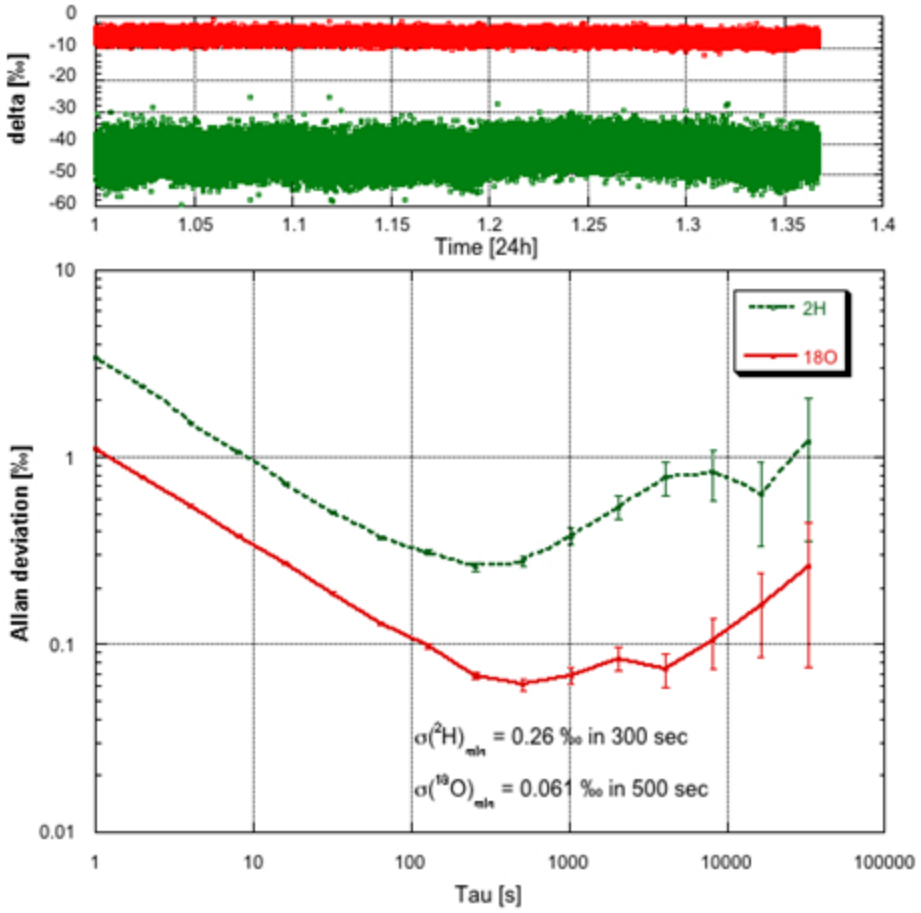

Figure 5. Time series of $\delta^{18}O$ (upper trace, top panel) and $\delta^{2}H$ (lower trace, top panel) and the Allan-Werle plot (lower panel) for data obtained under the conditions described in the text, notably a water concentration of ~10,000 ppmv.

2.4 Liquid water evaporator

An evaporator unit was built in order to completely vaporize the liquid water samples and to subsequently transport the vapour to the isotope analyzer. The evaporator (see Figure 6) consists of an evaporation chamber (~500cc) with a three-port cap, two on/off valves, two proportional valves, and a pressure meter. A dry carrier gas such as nitrogen is connected to the injection port of the chamber through the inlet on/off valve. The nitrogen supply line is also connected to the input of the gas analyzer through one proportional valve to allow for a dry nitrogen flow to be sent to the cavity. The input port of the chamber, through which liquid water samples are injected into the chamber, is sealed with 12 mm PTFE/silicone septa (Screening Devices BV, The

Netherlands). The output port is connected through a 4-way connector to the cavity through a proportional valve to control the flow of water vapour to the cavity, to a small vacuum pump through an on/off valve which enables full evacuation of the evaporator, and to a pressure meter to monitor pressure inside the chamber (STS ATM 1ST). An over-pressure relief-valve for an absolute pressure between ~1.5 and 2 bar is used in the nitrogen inlet line as an additional protection. The interior surfaces of the stainless steel tubes of the flash evaporator are fused silica coated (O'Brien).

The chamber is heated using a rubber band heater (Minco) in direct contact with the outside wall of the chamber. An on-off temperature controller (Minco) regulates the chamber temperature at ~140° C. This assures that the microliter water quantity injected into the chamber evaporates completely thus avoiding isotopic fractionation: the water vapour will have exactly the same isotopic composition as the liquid from which it was derived. The proportional valves of the unit are controlled with the OF-CEAS program in communication with the ARM9 microcontroller on the AP2E spectrometer mother board. The pressure sensor of the chamber is read out by a 16-bit ADC. Two on/off valves (one at the exit end of the chamber and another one at the inlet port of the chamber; Fig 6) and the autosampler are also controlled by the computer. For more technical details we refer to the internal report of M. Thijs [16].

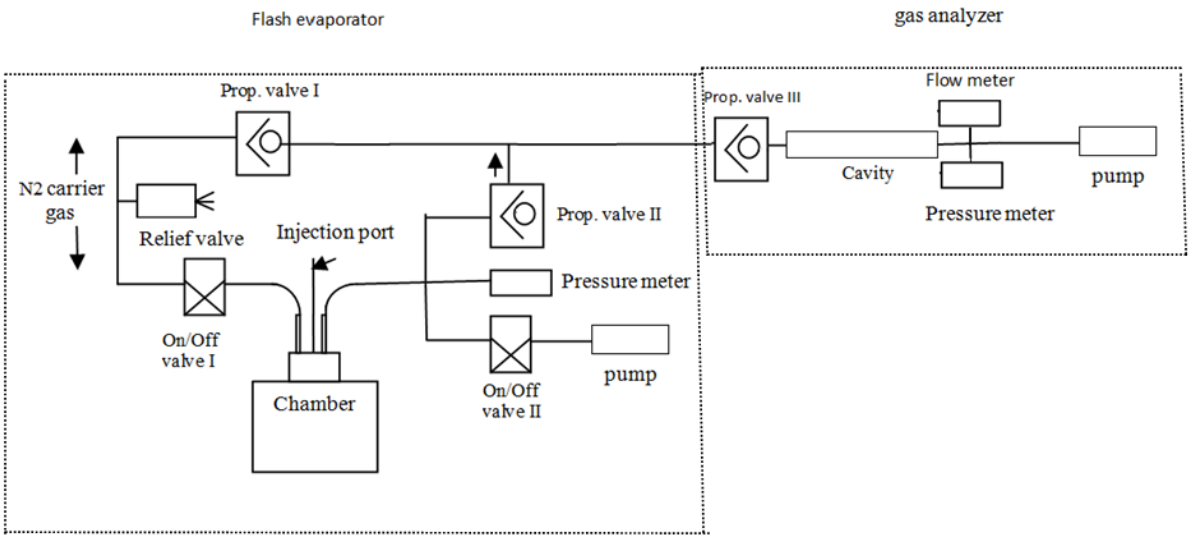

Figure 6. Schematic of the evaporator for complete vaporization of liquid water without isotopic fractionation.

2.5 Autosampler

The gas analyzer and the liquid evaporator are coupled with a CTC GC PAL liquid autosampler (CTC Analytics AG, Switzerland) to make periodic automated measurements of liquid water samples. The autosampler is controlled by the computer. The autosampler is programmed to retrieve the desired amount of water from 2-mL septum screw-capped glass vials. Repeated retrieval of water from a single vial will lead to multiple punctures of the septa and may eventually cause leaks, therefore septa should have excellent resealing capabilities. We used an 8-mm diameter cap and septum combination seal (Aluglas 1013688) for this purpose.

We tested 5-µL volume glass syringes with a fixed needle, as well as 10-µL syringes with a removable needle (both from SGE Analytical Science), for the same injection volumes. The accuracy and reproducibility of the delivered sample volume was found to be identical for both models. However, the 5-µL syringes have a stainless steel plunger which clogged fast and could not be interchanged or replaced if damaged, while for the 10-µL syringe needle clogging occurred after only ~2000 repeated injections, at which time the needle could be easily removed and replaced. Therefore, we preferred to use the more robust (and in the long run cheaper) 10-µL syringe. After each measurement series (about 100 injections), a manual cleaning of the needle was performed by placing it in an ultrasonic bath with deionised water.

2.6 Measurement procedure

The measuring process is fully automatic. Code has been incorporated into the main OF-CEAS program to control components of the evaporator unit (Figure 6) and to interact with the autosampler. A measurement cycle starts with the opening of the valve at the exit end of the chamber (On/Off valve II in Figure 6), in order to evacuate the chamber. Thus, when the evacuation is completed the chamber exit valve (II) is closed. Then a water injection command is issued to the autosampler. This initiates two needle-rinsing cycles with the aim to reduce sample carry-over from one injection to the next. The wash water is dispensed to waste. When the full cleaning cycle is completed, the syringe collects the final water sample and injects it into the chamber through the injection port. The amount of injected water sample will be discussed in Chapter 3 (where we investigate the accuracy and precision for natural samples). Because the chamber is maintained at 140 ˚C and is under vacuum, water is instantaneously vaporized. All transfer lines of the flash evaporator are wrapped with heating tape to prevent condensation.

Water vapour is then diluted with N2 gas, which enters the chamber through the inlet port (On/Off valve I in Figure 6), until the set final pressure in the chamber is reached (~1 bar). The mixture is then allowed to stand for ~ 2 minutes to ensure a thorough mixing of the water vapour and the carrier gas. Figure 7 shows graphical representation of the measurement routine. During sample equilibration, the proportional valve I (shown in Figure 6) opens to allow the cavity and the tube in the flow path from the N2 supply to the cavity to be flushed with N2 gas to reduce memory of the previous sample. The dry N2 flow through the spectrometer is measured by the Honeywell electronic flow meter inside the instrument. After equilibration, the proportional valve I slowly closes, while proportional valve II slowly opens in such a manner that the flow rate through the spectrometer remains fixed at 30 ml min^{-1}. As can be seen in Figure 7, following the switch to the sample flow, a sharp increase of concentration is observed. This is because when water is evaporated in the chamber, a small portion of water vapour can enter the tube to the cavity through the outlet port of the chamber.

The isotopic ratio is then measured for 4 minutes during the flat part of the isotope ratio profile. A post-run clean up of the raw isotopic ratios is performed by deleting outliers that deviate more than ± 2.6 σ from the mean value of the run. For a total of about 1000 data points, a maximum number of 40 data points are rejected as outliers.

After the measurement period ends, the evaporator is disconnected from the gas analyzer. Next, the chamber is evacuated by on/off valve II at the exit end of the chamber (see Figure 7) and then closes in order to accept a new water sample. The complete measurement cycle time for each aliquot of a liquid sample equals about 15 min.

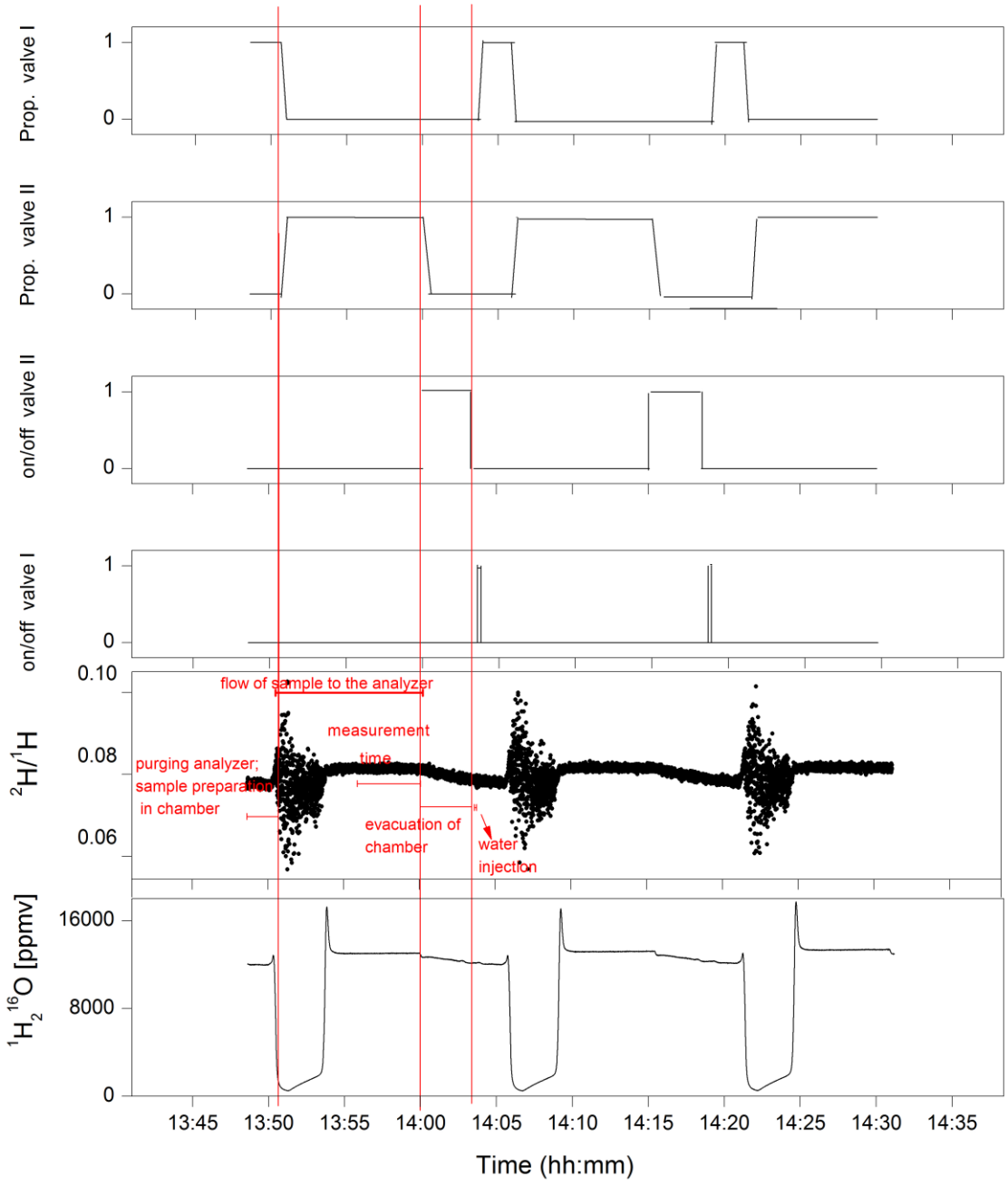

Figure 7. The valves diagrams, $^2H/^1H$ isotope ratio, and water concentration during three subsequent measurements of the same water sample with isotopic composition of δ^2H= -113.4 ‰ and $\delta^{18}O$ = -15.29 ‰ at 11000 ppmv water mixing ratio. The red vertical lines indicate the switching points to the next step. For further explanation see text.

2.7 Data acquisition and analysis

A C-program on the ARM9-based microcontroller is used to control the instrument, the data acquisition, and the on-line data processing. The OF-CEAS Labview program is used to communicate with the ARM9. Housekeeping data including cavity temperature and pressure, laser temperature, pressure in evaporation chamber, and nitrogen and water vapour flows are averaged over 10 consecutive acquisitions before being recorded in the housekeeping file. The two photodiode output signals are digitized using two 16-bit ADCs. The laser is scanned repeatedly at a scanning frequency of 4 Hz across approximately 120 successive longitudinal cavity modes spaced by 151.5 MHz (corresponding to ~ 0.6 cm^{-1}).

The absorption scale is calibrated by determining the ring-down time at the top of the last cavity mode transmission in the scan as explained in detail by Kerstel et al. [17] and Morville et al.[5]. To this end the laser is interrupted for approximately 1 ms at the end of each scan. A multiple-line fitting algorithm is used to retrieve concentrations and isotope ratios from the experimental spectra. The parameters in the fit are the line position, height, Lorentzian (collisional) width, Gaussian width, and Dicke collisional narrowing parameter, for each individual absorption line. The baseline is fit by a 3^{rd}-order polynomial and also includes a small sinusoidal oscillation associated with an optical fringe (interference) that is included in the fit. The intensity and phase of the fringe are free parameters while its frequency is fixed to a value determined off-line from a FFT (Fast Fourier Transform) analysis.

The Gaussian widths of all absorption lines are fixed to their calculated values (based on the gas cell temperature and isotopologue mass). The relative line positions, the pressure broadening (Lorentzian width) and Dicke coefficients were fixed to values determined previously for an exemplary measurement. Line grouping is used for weaker lines in the spectrum to fix the relative intensities of lines belonging to the same isotopologue. Since for a given set of fit parameters all line widths are fixed, the isotopologue concentrations are directly proportional to the line intensities. The proportionality factors were first calculated based on the line intensities reported by HITRAN, and then refined using repeated measurements of an isotope standard close to VSMOW (the Groningen working standard GS-48 with $\delta^{18}O$ =-6.51 ‰, $\delta^{17}O$ = -3.4‰, and $\delta^{2}H$ = -43.4 ‰, with respect to VSMOW). In this way, the instrument is capable of reporting fairly reliable “raw” isotope ratios (evidenced by near-unity slopes in the calibration graphs of Chapter 3).

If any additional absorption lines appear in the spectra, like methane absorption lines in atmospheric water vapour measurements or absorption features belonging to alcohols in liquid water analyses, they can be included in the fit [2]. For the purpose of the measurements carried out in the framework of this thesis, no such additional spectral features were needed.

Figure 8 shows a typical experimental spectrum recorded for a natural water with isotopic composition of δ^2H= -113.4 ‰ and $\delta^{18}O$ = -15.29 ‰ at 11,000 ppmv together with the fitted spectrum, and the residuals of the fit in the bottom panel. The RMS of the residuals of the fit is 2.4×10^{-9} cm^{-1} (at 4 Hz measurements), corresponding to a noise equivalent absorption sensitivity (NEAS) of 1.2×10^{-9} $cm^{-1}Hz^{-1/2}$. As may be clear from Figure 8, the NEAS is largely determined by the quality of the fit. The spectrometer NEAS, as determined from an empty gas cell spectrum, is equal to about 4×10^{-10} $cm^{-1}Hz^{-1/2}$, comparable to that obtained with previous spectrometers with a similar mirror reflectivity [14, 17].

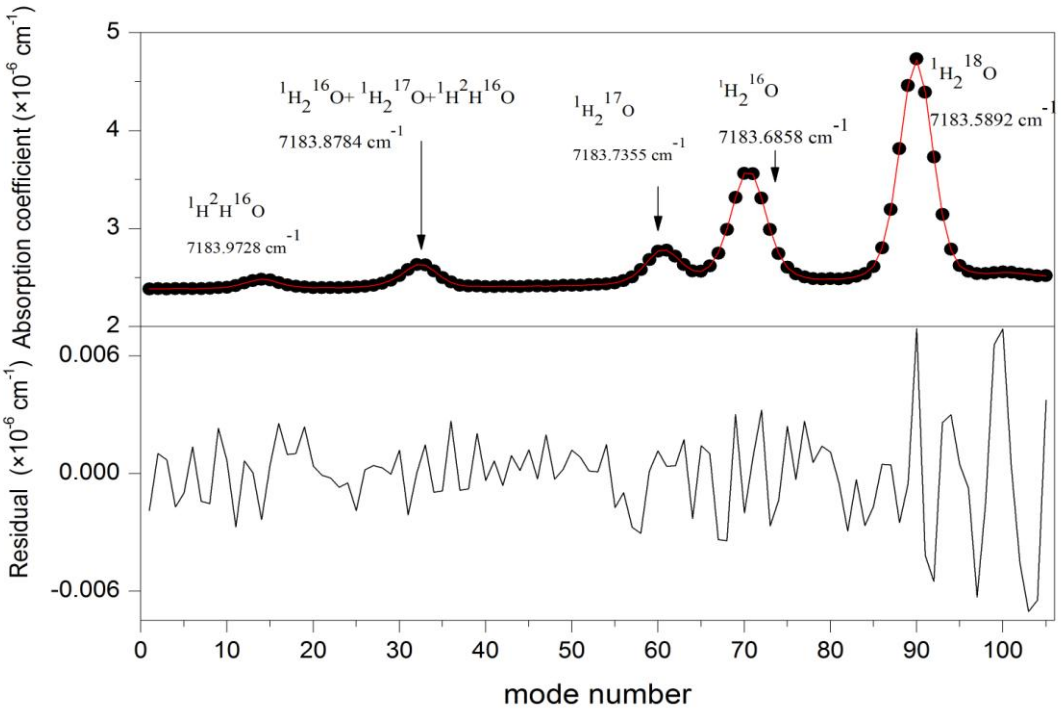

Figure 8. Experimental spectrum (black circles) and fitted spectrum (red curve) at 11000 ppmv water vapour mixing ratio (corresponding to the volume injection of 2.8 µL) of a natural water (δ^2H= -113.4 ‰ and $\delta^{18}O$ = -15.29 ‰). The RMS of the residuals (bottom panel) equals 2.4×10^{-9} cm^{-1}, and is limited by the fit.

References

[1] http://www.ap2e.com

[2] Landsberg J 2014 Ph.D. Thesis, J. Fourier University (Grenoble I) and University of Groningen

[3] Morville J, Kassi S; Chenevier M and Romanini D 2005 *Appl.Phys. B* **80** 1027

[4] Morvile J: Ph.D Thesis, J. Fourier University (Grenoble I)

[5] Morville J; Romanini D and Kerstel E 2014 Chapter 5 in (Gagliardi G and Loock H.P, Eds.) *Cavity-Enhanced Spectroscopy and Sensing*, Vol. 179. Springer Series in Optical Sciences, 163

[6] Kerstel E.R.T 2004 Chapter 34 in (de Groot P A, Ed.) *Handbook of Stable Isotope Analytical Techniques*, Vol. 1. Elsevier: Amsterdam, The Netherlands, 759

[7] Bergamaschi P, Schupp M and Harris G W 1994 *Appl. Opt*. **33** 7704

[8] Kerstel E R Th, Gagliardi G; Gianfrani L, Meijer H A J; van Trigt R and Ramaker R 2002 *Spectrochim. Acta A* **58** 2389

[9] Kerstel E and Gianfrani L 2008 *Appl. Phys. B* **92** 439

[10] Gianfrani L, Gagliardi G, van Burgel M and Kerstel E.R.Th 2003 *Opt. Express* **11** 1566

[11] Kerstel E R Th, van Trigt R, Dam N, Reuss J and Meijer H A J 1999 *Anal. Chem***. 71** 5297

[12] Dyroff C, Fütterer D and Zahn A 2010 *Appl. Phys. B* **98**, 537

[13] Rothman L S; Gordon I E; Babikov Y, Barbe A, Chris Benner D, Bernath P F, Birk M, Bizzocchi L, Boudon V, Brown L R, Campargue A, Chance K, Cohen E A, Coudert L H, Devi V M , Drouin B J, Fayt A, Flaud J-M, Gamache R R, Harrison J J, Hartmann J-M, Hill C, Hodges J T, Jacquemart D, Jolly A, Lamouroux J, Le Roy R J, Li G, Long D A, Lyulin O M, Mackie C J, Massie S.T, Mikhailenko S, Müller H S P, Naumenko O V, Nikitin A V, Orphal J, Perevalov V, Perrin A, Polovtseva E R, Richard C, Smith M A H, Starikova E, Sung K, Tashkun S, Tennyson J, Toon G C, Tyuterev Vl G and Wagner G 2013 *J. Quant. Spectrosc. Radiat. Transfer* **130** 260

[14] Iannone R Q, Kassi S, Jost, H J, Chenevier M, Romanini D, Meijer H A J, Dhaniyala S, Snels M and Kerstel E R T 2009 *Isotopes Environ Health Stud*. **45** 303

[15] Werle P, Mucke R and Slemr F 1993 *Appl. Phys. B: Photophys. Laser Chem* **57** 131

[16] Thijs M 2012 Report Internship, J. Fourier University (Grenoble I)

[17] Kerstel E, Iannone R Q, Chenevier M, Kassi S, Jost H J and Romanini D 2006 *Applied Physics B-Lasers and Optics* **85** 397